Regulation and recycling of myosin V

Kenneth A Taylor

Recently there has been considerable progress in our understanding of regulation for unconventional myosin-V through elucidation of the structure of its inactive conformation and the factors that affect stability of this conformation. The inactive conformation is a folded compact structure characterized by interactions between the myosin head and the C-terminal cargo binding domain. Concentrations of Ca^{2+} greater than 10 μM disrupt folding. The 3-D structure determined by cryoelectron tomography of 2-D arrays in one study and electron micrographs of isolated molecules reported in another reveal similar features, but suggest different F-actin affinities for the inactive conformation. This has raised the question of how inactive myosin-V is recycled to other sites for additional rounds of cargo transport.

Addresses
Institute of Molecular Biophysics, Florida State University, Tallahassee, FL 32306-4380

Corresponding author: Taylor, Kenneth A (taylor@bio.fsu.edu)

Current Opinion in Cell Biology 2007, **19**:67–74

This review comes from a themed issue on
Cell structure and dynamics
Edited by Daniel P Kiehart and Kerry Bloom

Available online 8th January 2007

0955-0674/$ – see front matter

DOI 10.1016/j.ceb.2006.12.014

Introduction

The most widely pursued questions regarding the function of molecular motors pertain to the active state: the degree to which it is processive, its step size and speed, and what kind of cargo is transported. Equally important, however, is the mechanism by which the motor is turned off and how effectively the ATPase activity is inhibited. The kinetic state in which the inhibited conformation is trapped is also important because this will determine the affinity of the inhibited form for its track.

Related to the question of regulation is the concept of motor recycling; once the motor reaches the end of its filament track, how is it inactivated and returned to a plausible starting position for another active cycle? For most cytoplasmic motors, the existence and structure of an inactive conformation is unknown. Moreover, it is usually assumed that the inactive motor simply diffuses passively to a new location. Other mechanisms to accomplish this goal include more active return via a companion but oppositely directed motor, or via treadmilling or retrograde movement of the motor's track.

The two families of microtubule-based motors move in opposite directions; the kinesins are largely plus-end directed, whereas the dyneins are minus-end-directed, thereby permitting one family to act as the retrograde transporter of the other. Among myosins, all but one are plus-end directed; only myosin VI is known to be minus-end directed. Although it is possible that other minus-end directed myosins may be found, it remains likely that they will be rare. Thus, myosin recycling is possibly more complex than it is for microtubule based motors.

This review discusses recent progress toward understanding regulation of myosin-V, the most extensively studied of the 'cargo carrying' unconventional myosins, and the structure of its inactive conformation. It then explores the question of myosin-V 'recycling', or, to put it in a different way, how to return myosin-V to a plausible starting position for reuse.

Myosin-V regulation

Myosin-V is found in a wide variety of eukaryotic organisms and is involved in diverse cellular processes, such as vesicle, mRNA and melanosome transport (reviewed by [1]). Myosin-V has two heavy chains folded into an obligate dimer. Each heavy chain forms a motor domain, which contains the catalytic and actin binding activities, followed by a neck region that consists of a long α-helix containing six tandem IQ motifs with the sequence IQxxxRGxxxR, each of which binds calmodulin (CaM) or a CaM-like light chain that stiffens the α-helix into a lever arm (Figure 1a). These 'head' and neck domains are connected to a largely α-helical coiled-coil tail domain interrupted by two disordered domains. A cargo binding domain (CBD) occupies the C-terminus. Some isoforms of myosin V can bind one class of dynein light chain at a location within the second of the two disordered domains of the tail (Figure 1a) [2]. A number of laboratories have established that the myosin-V dimer is a processive motor with a step size equal to the crossover repeat of the F-actin filaments, 36 nm, on which it walks.

Initial characterization of chicken brain myosin-V showed a large increase in ATPase activity on addition of F-actin as well as an effect of $[Ca^{2+}]$ on both ATPase and motility [3]. In EGTA, addition of F-actin increased ATPase activity by 25–30 fold but in 10 μM $[Ca^{2+}]$, actin activated ATPase activity increased ~200 fold. This modest (approximately eight-fold) effect of $[Ca^{2+}]$ has been observed in numerous laboratories and suggested ATPase

Figure 1

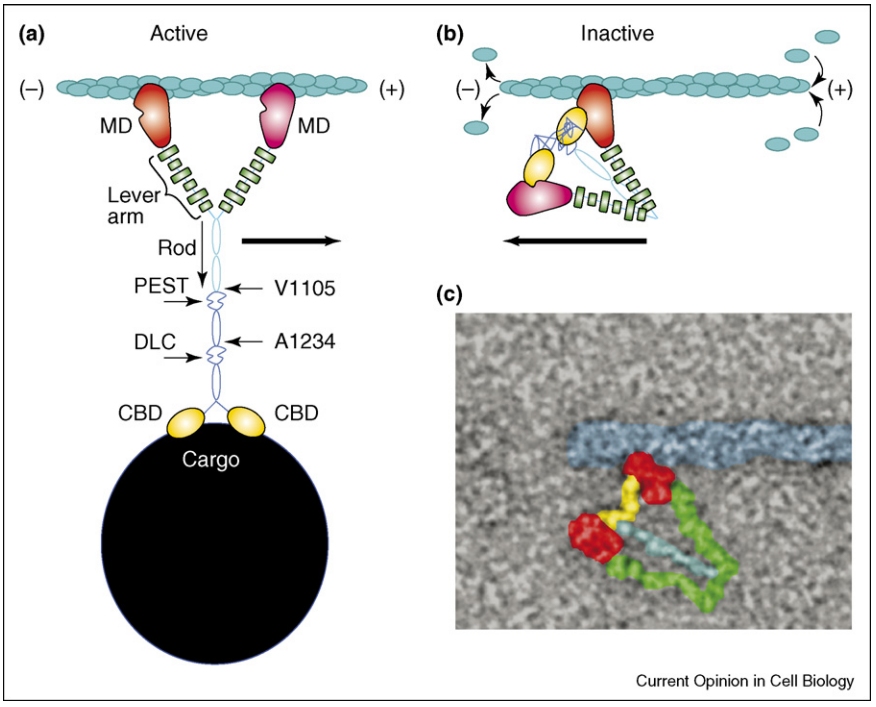

Diagram of myosin-V in the active and inactive 14S conformation. **(a)** This shows a schematic view of active myosin-V with a vesicle bound to the cargo binding domain (CBD). Actin is light blue. Each myosin-V heavy chain has a motor domain (MD; red) and a lever arm (cyan) that has six calmodulin light chains (green) bound. An elongated rod domain has three predicted coiled-coil segments; the first (cyan) is broken at the PEST site, which begins at residue V1105, the second (blue) after residue A1234, the third (blue) extends to the CBD. The dynein light chain, labeled DLC, binds within the second uncoiled region. **(b)** Myosin-V in the inactive conformation folds up using interactions between the CBD and the motor domain. Binding to actin is limited to one head per actin filament. The structure has an asymmetric placement of the first coiled-coil segment relative to the CBDs. This might allow for further folding of the rod along the paired CBDs as suggested in reference [32]. If the inactive conformation binds actin strongly, it will stay bound while actin monomer addition to the (+) end displaces the actin filament toward the (–) end. **(c)** Electron micrograph of folded myosin-V bound to actin showing single headed actin binding. Same coloring scheme as in (b). Adapted from reference [23].

activity might be regulated. Surprisingly, in 10 μM [Ca^{2+}], where steady state ATPase assays showed high activity, *in vitro* motility assays showed reduced actin movement. This calcium effect on motility is now thought to be due to dissociation of one or more CaM from the myosin-V lever arm because addition of ~10 μM excess CaM rescues motility even in 10 μM [Ca^{2+}] but does so only partially [3,4•,5]. CaM dissociation would cause the lever arm to become too flexible to communicate strain between forward and trailing heads, thereby disrupting processive movement [6].

In standard motility assays where the myosin-V is immobilized on a nitrocellulose substrate and the F-actin filament is allowed to move, full length myosin-V moves F-actin filaments as well or better in EGTA as in high [Ca^{2+}] [3,7–10]. This effect is thought to be due to unfolding of the inhibited conformation by the immobilizing nitrocellulose. Recent studies using TIRF, in which the F-actin filament is held stationary on the substrate and the myosin-V allowed to move, have supported this interpretation [11••]. Shortening of myosin-V processive runs was observed at [Ca^{2+}] as low as 1 μM with progressive shortening as [Ca^{2+}] increased to 100 μM. The effect is observed in both a regulated, full length construct and an unregulated two-headed HMM construct. Movement, albeit shorter, was observed in ~12% of full length constructs even in EGTA, a proportion of activated molecules consistent with the eight-fold increase in steady state actin activated ATPase activity in 10 μM [Ca^{2+}]. Thus, transient dissociation of CaM can terminate a processive run.

Small amounts of unregulated protein can have a large effect on steady state ATPase assays of an inhibited state. Highest levels of regulation are usually obtained using single turnover kinetic measurements, where each molecule contributes only one cycle to the measurements. With such methods, the highest levels of regulation observed for myosin-V are 50-fold [11••]. By comparison, in smooth muscle myosin-II, a species that is regulated by phosphorylation of its regulatory light chain (RLC) rather than Ca^{2+} binding but which like myosin-V also folds into a compact conformation in its inhibited state (for a review

see [12]), the levels of inhibition can be as high as 1000-fold [13]. Thus, myosin-V exhibits relatively poor inhibition compared with some myosin-II species. Other, as yet undetermined, factors may contribute to the regulation *in vivo* but in the absence of such unknown factors, it remains to be determined whether or not the observed levels of regulation are sufficient to account for myosin-V behavior in living cells.

Myosin-V has unusually strong affinity for F-actin in its weak binding kinetic intermediates. Virtually all of a suspension of full length myosin-V sediments in 0.3 μM actin, 13 μM [Ca^{2+}] and ATPγS, a non-hydrolyzable analog of ATP [14]. Under the same conditions but in EGTA, very little myosin-V sediments with actin. The myosin-V–F-actin affinity in the weak binding states was recently investigated using ATPγS and two mutations in the switch II region that eliminated ATP cleavage but not ATP binding [15]. The dissociation constant for actin binding in 50 mM KCl with ATPγS was 13 μM, while the switch II mutations trapped two distinct states, one with a K_D for actin binding of ~2 μM and the other with a K_D of ~0.2 μM. These F-actin affinities are 100–1000 fold higher than myosin-II in ATPγS for which the dissociation constant from F-actin is ~1 mM at physiological salt concentration [16]. By comparison, the K_D for myosin-V–F-actin binding in ADP is 7.6 nM [17].

Effects of Ca^{2+} and calmodulin on myosin V

The six IQ motifs of the myosin-V lever arm, while highly conserved, are not identical in sequence therefore allowing a complex response to changes in [Ca^{2+}]. Ca^{2+} binding can increase the affinity of CaM for some myosin-V IQ motifs and decrease the affinity for others [18]. In addition, crystal structures of the CaM-like light chains from myo2p, a myosin-V isoform from *Saccharomyces cerevisiae*, show two conformations, one that is closed with both lobes binding the IQ motif and another, open conformation with the N-terminal lobe dissociated from the IQ motif [19]. Thus, detachment of only one lobe of CaM from the IQ motif is possible without complete dissociation. Both dissociation and single lobe detachment by a CaM would increase flexibility in the lever by increasing the length of unstabilized α-helix.

Between one and two CaMs are thought to be dissociable from each myosin-V lever arm. Several studies observed CaM dissociation from IQ2, which is generally complete in 10 μM [Ca^{2+}] [4•,8,20], while another shows that CaM affinity for IQ2 is the weakest of the six motifs in myosin-V [18]. One study at variance to these results identifies CaM dissociation from IQ6 [9], which is nearest the junction between the two heads. CaM dissociation from IQ2 would probably be more effective than dissociation from IQ6 in uncoupling conformational changes in the motor domain from the rod domain and companion head because of the greater reduction in effective lever arm length.

Although complete dissociation would be the most effective for changing the lever arm stiffness, and could account for observations in which added CaM only partially restores motility, dissociation by one lobe of CaM could provide an intermediate level of response. One suggested possibility is the binding of CaM across two IQ motifs [18], an event that would produce a dramatic change in lever arm direction if one CaM lobe detached adjacent to an IQ motif with no bound CaM. However, this has not yet been visualized directly by EM. Another possibility is binding of another protein by the detached CaM lobe [19].

Structure of the myosin V inactive state

Three groups have studied the structure of the myosin-V inhibited conformation, and all have reached a similar conclusion; the inhibited (off-state) involves folding from an open, active conformation, which has a sedimentation coefficient of ~10S, into a closed, inhibited conformation that sediments at 14S [4•,20,21•,22•]. The 14S conformer is formed only by full length myosin-V, and does not require binding by the dynein light chain. The 14S conformer is stabilized in EGTA and disrupted by [Ca^{2+}] in excess of 10 μM, even in the presence of 6 μM excess CaM added to prevent dissociation [4•]. This implies that a structural change in CaM while still bound to the lever arm, such as dissociation of one lobe, is sufficient to disrupt folding of the 14S structure.

The first 3-D images of the 14S structure were recently obtained from paracrystalline 2-D arrays formed on a lipid monolayer [23••]. These were obtained using the new technique of cryoelectron tomography [24•]. The resolution of the 3-D image was 2.4 nm, which was sufficient to provide an envelope into which crystal structures of the motor domain, lever arm and a coiled-coil α-helix model could be placed. The result showed that the postpower stroke lever arm orientation typical of strong F-actin-binding states fits the reconstruction best. This was confirmed by decorating F-actin at low protein concentration. F-actin binding by only one head was seen in these images (Figure 1c). Neither head is sterically blocked for actin binding, but the 14S conformation restricts both heads from binding simultaneously. Binding to two actin filaments ~24 nm apart would not be restricted.

The CBD density was juxtaposed with loop 1 of the motor domain (Figure 2), a structure that in myosin-II is known to modulate the rate of nucleotide binding and release [25], suggesting that ATPase inhibition was due to reduced rates of nucleotide exchange. This suggestion has found support from studies of ADP release by full length myosin-V, which showed that in EGTA, ADP release was slowed even in the presence of F-actin [11••,26••]. On the other hand, ATP binding to nucleotide-free, full-length myosin-V (presumably in the folded,

Figure 2

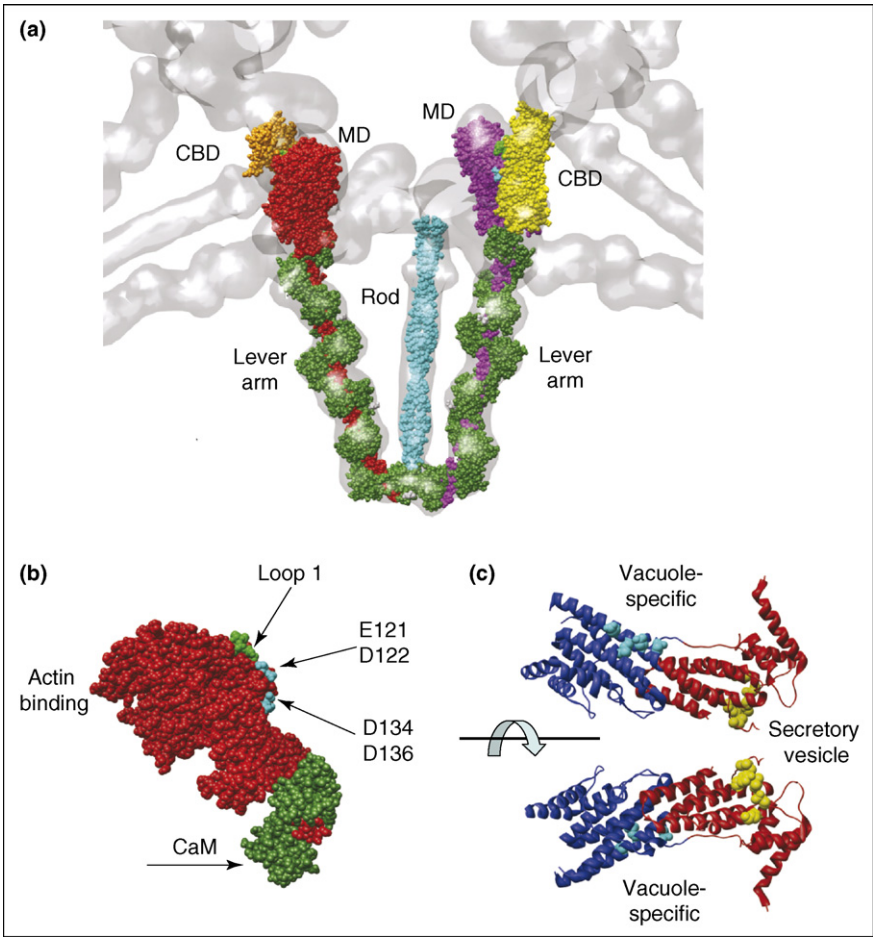

(a) Image of the Liu *et al.* 3-D reconstruction of the inactive conformer of myosin-V [23••] with the crystal structure of the CBD [31••] modeled in. The two CBDs, colored yellow and orange, and are placed between the motor domains, colored red and magenta. These CBDs probably come from adjacent molecules through domain swapping. In (a) and (b), the regions of the motor domain involved in CBD interaction are colored green (loop 1) and two other sites [27••] are colored cyan. These sites all occur on the same side of the motor domain. The CBD can be modeled into the map density in numerous ways, but the one shown comes near to both sets of interaction sites. The CaM light chain bound to IQ1 is colored green. **(b)** Higher magnification view showing the relationship of the CBD interaction sites with the actin binding surface. **(c)** Yeast CBD crystal structure shown as a ribbon diagram for the two domains (domain 1 in blue; domain 2 in red). Those residues involved in vacuole-specific interactions on domain 1 are rendered in space filling and colored cyan; those residues involved in secretory vesicle transport (domain 2) are rendered in yellow. Note that these two regions are placed on opposite sides of the CBD.

14S conformation) shows no [Ca^{2+}] dependence. This implies that if folding to the 14S conformation occurs with ADP bound in the active site, which *in vivo* would occur while actin bound, exchange of ATP for ADP will be slowed. Biochemically, strong F-actin-binding by the 14S structure in ADP was found to be limited to a single head [26••], a result in agreement with the structural studies.

A second study [27••] reported averaged projections from electron micrographs of negatively stained specimens of the 14S myosin-V conformation. They also concluded the 14S conformation was stabilized by a CBD-motor domain interaction but at a different site on the motor domain (Figure 2a,b). They went on to show that when an HMM fragment of myosin-V that lacked the CBD was incubated with an exogeneous dimeric CBD, it could produce a structure similar in conformation to the 14S particle formed from intact myosin-V. In contrast to the studies mentioned above, the conditions used here produced a 14S conformation with weak F-actin affinity consistent with a prehydrolysis state with bound but uncleaved ATP. In agreement with this, they were unable to decorate F-actin at low F-actin concentrations.

The 14S conformation can be formed in the absence of nucleotide, in ADP and with ATP [4•,23••,27••]. Ironically, all three states correspond to conformations with the post-powerstroke lever arm orientation, but they each have dramatically different affinities for F-actin. In 50 mM KCl, the corresponding myosin-V affinities for

actin are 4.9 pM, 7.6 nM and13 μM (ATPγS), respectively [15,17]. Which is most important *in vivo* depends on which dominates in the steady state and that may depend on whether folding occurs with ADP bound in the active site.

Identical 2-D arrays of myosin-V form in ADP with or without 20 mM inorganic phosphate. Under similar conditions of ADP and phosphate, smooth muscle myosin-II folds into a closed, inactive form with a prepowerstroke lever arm orientation. [28,29] A similar result was expected with myosin-V. That 20 mM inorganic phosphate seems to have no effect on the 14S structure suggests that the folded myosin-V conformation is highly specific for lever arm orientation.

Superficial comparison of the two structures suggests that the conformation in the arrays, although unambiguously a folded conformation, is different from the one observed in individual molecules (Figure 2). The high protein concentrations produced in ordered arrays facilitates the interchange (swapping) of domains between adjacent molecules and this would occur if it led to a more stable structure (this is a common crystallization artifact [30]). It is therefore possible that the close proximity of myosin-V motor domains and CBDs among adjacent molecules in the arrays is facilitating intermolecular interactions. This is not expected to change how the domains interact with each other. Based on their different relative degrees of ATPase inhibition, the 14S conformation is not as stable as the folded inhibited structure of dephosphorylated smooth muscle myosin II and HMM, for which domain swapping did not occur in 2-D arrays [28,29]. This effect may also underlie the strong F-actin affinity observed for myosin-V in ATP and high [Ca^{2+}] [14], conditions that would prevent folding to the 14S conformation, but not intermolecular head–CBD interactions. *Inter*molecular head–CBD interactions would provide cooperative effects in actin-bound myosin-V that are not observed with isolated molecules in the folded, 14S conformation, which is characterized by *intra*molecular head–CBD interactions.

The structure of the CBD from yeast myosin-V has recently been solved [31••]. The structure consists of two five-helix bundles that share one long α-helix (Figure 2c). The overall dimensions are 9.5 x 2.5 x 3.0 nm. The five helices of each subdomain are largely oriented along the long axis. Each subdomain has two or three additional small α-helices. Yeast myosin-V is involved in both vacuole inheritance as well as secretory vesicle transport. The requisite binding activities are localized to opposite sides of the separate subdomains.

Interactions between the myosin-V rod and its CBD were examined using HMM constructs with rod domains truncated to different lengths in the presence of exogeneous, monomeric CBD [32••]. The segment of the initial coiled-coil between V1105 and A1234 (Figure 1a) was found to be critical to obtain regulation while segments closer to the CBD were not. Because the CBD construct behaved as a monomer, whereas in the 14S conformation the two CBDs are closely juxtaposed, a plausible explanation is that the critical rod regions may be facilitating dimerization of the CBD monomers, which is necessary to stabilize the closed conformation. This region includes two segments of coiled-coil separated from the first segment by what is called the PEST site. In both of the EM studies [23••,27••], the initial segment of rod lies closer to one myosin-V head and its CBD than the other. It may be that the rod domain placement incorporates a 90° change in direction at the CBD, thereby enabling rod α-helices to line up parallel with CBD α-helices, which would increase the potential for stabilizing interactions.

Myosin-V recycling on treadmilling F-actin

Myosin-V is localized to sites where F-actin is turning over rapidly [33–35]. F-actin concentration is high in these locations and the filaments are uniformly oriented with plus-ends towards the plasma membrane. Once myosin-V reaches the plus-end, it will presumably remain there until its cargo unloads and it can fold into the inactive conformation. If it is to be reused, it must be returned by some mechanism to the beginning of the track or some other location where needed. Diffusion is one possibility. However, for 14S myosin-V to diffuse efficiently, it must have very low affinity for F-actin which does not appear to be the case. Another possibility is transport of myosin-V to a new location but this would require colocalization with myosin-VI, which is not generally observed. Transport along microtubules by cytoplasmic dynein would be important for long distance recycling, but would not help myosin-V escape dense actin matrices, which usually exclude microtubules. Kinesin transport of myosin-V will generally move it toward the cell periphery, the same direction it would move actively on actin (reviewed in [36]).

Retrograde actin flow or actin treadmilling provides an alternative to a companion motor or simple diffusion (Figure 1b). The relative importance of retrograde transport on treadmilling actin filaments compared to diffusion depends on the lifetime of the actin attached state. The molecule's facility for diffusion to the minus-end depends on the lifetime of the actin detached state, which in turn depends on the actin concentration and the actin bundle environment (Box 1).

There is currently disagreement over the F-actin affinity of the closed 14S conformation of myosin-V [23••,27••]. Actin binding appears to be possible for only one of the two myosin-V heads, but if that head has •ADP bound, its lifetime could be ~30 sec, allowing ~3 μm of retrograde movement (Box 1). On the other hand, actin-bound myosin-V in the prehydrolysis ATP state would have a

Box 1 Diffusion versus treadmilling

The balance between diffusion and retrograde flow depends on (a) diffusion coefficient, D, (b) actin concentration, (c) lifetime of the detached state, t_{det}, (d) lifetime of the attached state, t_{att}, and (e) valency, which is 2 for myosin-V. The diffusion coefficient of myosin-V is not known, but for spherical volumes, it scales with the cube root of the molecular weight (MW). Using the diffusion coefficient for G-actin, MW 42 kDa, is 5 μm^2/sec [40], the diffusion coefficient of dimeric myosin-V, MW 608 kDa, would be about 2 μm^2/sec. This is probably an overestimate because 14S myosin-V is not spherical, although it is relatively compact.

Myosin-V localizes to regions of high actin turnover indicative of active treadmilling. In these regions, the F-actin concentration is high, but not precisely known and difficult to estimate as the filament arrangement is not precise. For active myosin-V to operate within a dense actin network might require an ~40 nm interfilament spacing, which is a spacing typical for crosslinking by α-actinin, a relatively long F-actin crosslinker. A hexagonal array of actin filaments with 40 nm interfilament spacing would have an F-actin concentration of 435 μM. By comparison, the F-actin concentration in some striated muscles, such as insect fibrillar flight muscle, is 770 μM. In the 14S conformation, myosin-V could bind two actin filaments spaced ~24 nm apart. The F-actin concentration would then be 1.2 mM.

Lifetimes for the attached (A M·nucleotide) and detached (M·nucleotide) states can be predicted from the forward (k_+) and reverse (k_-) rate constants that comprise the dissociation constant (K_D). These are usually measured for single-headed constructs with one or two IQ motifs with CaM bound making them appropriate for 14S myosin-V. These are known for myosin-V ADP in 50 mM KCl [17].

$$A\,M^{\bullet}ADP \rightleftharpoons A + M^{\bullet}ADP \qquad KD = 7.6\,nM \tag{1}$$

$$d[M^{\bullet}ADP]/dt = k_+[AM^{\bullet}ADP] \qquad k_+ = 0.032\,sec^{-1} \tag{2}$$

$$d[AM^{\bullet}ADP]/dt = 2k_-[A][M^{\bullet}ADP] \qquad k_- = 4.2\,\mu M^{-1}\,sec^{-1} \tag{3}$$

$$\text{Diffusion distance} = 2(Dt_{det})^{1/2} \tag{4}$$

The factor 2 in Equation (3) is needed because myosin-V has two heads. The inverse of forward rate constant gives the attached state lifetime, t_{att} = 31.25 sec. The reverse rate constant times the F-actin concentration, 435 μM, gives the detached state lifetime, t_{det} = 0.27 msec. The corresponding forward rate constant for myosin-V in ATP has been measured in 100 mM NaCl (k_+ = 850 sec^{-1}) but not the reverse rate constant [8]. Assigning an equilibrium constant of K_D = 100 μM, based on an eight-fold increase due to the higher ionic strength (see below) and a K_D of 13 μM in 50 mM KCl [15], gives a reverse rate constant of k_- = 8.5 μM^{-1} sec^{-1}. The lifetime of the attached state would be t_{att} = 1.2 msec and for the same actin concentrations, t_{det} = 0.13 msec. This estimate for the detached state lifetime is rather unsatisfactory as it involves both an extrapolation for the salt effect (see below) as well as a mixture of experimental conditions, one of which measured K_D using ATPγS whereas the other measured k_+ in ATP.

Rates of actin retrograde flow are ~100 nm/sec [41] which gives a distance of 3.1 μm for myosin-V·ADP movement by retrograde flow while attached to actin. This would allow myosin-V to move almost the length of the leading edge, about 5 μm, in one attachment. For myosin-V·ATP the movement would be insignificant, only 0.12 nm.

The diffusion distance (Equation 4) for myosin-V·ADP while detached from actin is 10 nm. For myosin-V·ATP the distance would be 33 nm, based on the assumption given above. Diffusion would dominate for myosin-V·ATP, but would be in any direction. Note that diffusion distance scales as the square root of the change in actin concentration. Thus, for 24 nm interfilament spacing, diffusion distance would be 6 nm and 20 nm for the myosin-V·ADP and myosin-V·ATP states.

Other contributing factors are cooperative effects on myosin-V actin binding and the effect of ionic strength on the rate constants. Filament spacings near 24 nm would allow for 2-headed, 2-filament binding within the actin meshwork and cooperative effects, ignored here, would then become important. At the same time, such a dense actin network might limit the active state of myosin-V to the periphery the filament network.

K_Ds are generally salt dependent, especially for the weak binding states. For the myosin-V·ADP state, in 50 mM KCl the equilibrium constant is K_D = 7.6 nM [17] and in 100 mM NaCl, K_D = 61 nM [8], which is an eight-fold increase in K_D for a two-fold increase in ionic strength.

lifetime of 1 msec; retrograde motion would be insignificant compared to that of diffusion. Nevertheless, the time that myosin-V would spend bound to actin in high actin concentration would be 10 times as long as the time spent detached from actin. This would slow the rate of diffusion to about three times that of treadmilling for the same distance. Moreover, in the absence of a concentration gradient, diffusion would be unbiased with respect to any direction not blocked by the plasma membrane, whereas treadmilling is always in the same direction.

Retrograde movement of myosin-V has not been reported. On the other hand, dramatic fluorescent microscopy images of myosin-X movement along filopodia have been reported [37]. Myosin-X exhibits rapid anterograde flow toward the filopodium tip and slower retrograde flow toward the cell body, a phenomenon that has been named intrafilopodial motility. Filopodia have much more favorable actin bundle geometry for visualization than lamellapodia, but the structure of the retrograde moving myosin-X is unknown. However, many of the relevant rate constants have been measured [38•] and these show that myosin-X affinities for F-actin in the strong actin binding states are roughly comparable to the weak binding states of myosin-V.

Conclusions

The structure and characteristics of the inhibited state of myosin-V fits well into the emerging theme in which inactive states of cytoplasmic motors are characterized by folded conformations involving interactions between the CBD and the motor domain, as in myosin-V, or regions

close to the motor domain, such as the neck coiled-coil in kinesins (reviewed by [39]). Kinesin inactive states appear to be weak microtubule binders, consistent with recycling via diffusion or dynein transport. On the other hand, the inhibited conformation of myosin-V can be formed under conditions of widely different actin affinity. Consequently, the recycling mechanism is not as clear. Treadmilling and retrograde F-actin flow provides a mechanism for recycling myosin-V within locations where the F-actin concentration is high and diffusion would be retarded due to myosin-V's relatively high actin affinity even in the weak binding states. Ultimately, the importance of treadmilling for *in vivo* function of myosin-V can best be established by direct visualization, as has been done for myosin-X. Other unresolved issues include the circumstances under which myosin-V releases cargo and its catalytic state when folding occurs *in vivo*. Finally, there is the question of why myosin-V is poorly regulated relative to other myosins. Are there other as yet undiscovered factors? There is still much to be discovered in the regulation and recycling of cytoplasmic myosins.

Acknowledgements

The assistance of Jun Liu and Cheri Hampton in the production of figures is gratefully acknowledged. The author's research on myosin-V was supported by grant AR47421 from National Institutes of Arthritis, Musculoskeletal and Skin Diseases. Comments by Kathy Trybus, Hailong Lu and P Bryant Chase are gratefully appreciated.

References and recommended reading

Papers of particular interest, published within the annual period of review, have been highlighted as:

- • of special interest
- •• of outstanding interest

1. Reck-Peterson SL, Provance DW, Mooseker MS, Mercer JA: **Class V myosins**. *Biochim Biophys Acta* 2000, **1496**:36-51.

2. Hodi Z, Nemeth AL, Radnai L, Hetenyi C, Schlett K, Bodor A, Perczel A, Nyitray L: **Alternatively spliced exon B of myosin Va is essential for binding the tail-associated light chain shared by dynein**. *Biochemistry* 2006, **45**:12582-12595.

3. Cheney RE, O'Shea MK, Heuser JE, Coelho MV, Wolenski JS, Espreafico EM, Forscher P, Larson RE, Mooseker MS: **Brain myosin-V is a two-headed unconventional myosin with motor activity**. *Cell* 1993, **75**:13-23.

4. • Krementsov DN, Krementsova EB, Trybus KM: **Myosin V: regulation by calcium, calmodulin, and the tail domain**. *J Cell Biol* 2004, **164**:877-886.
This is one of three studies that initially characterized the inactive conformation of myosin-V.

5. Nguyen H, Higuchi H: **Motility of myosin V regulated by the dissociation of single calmodulin**. *Nat Struct Mol Biol* 2005, **12**:127-132.

6. Veigel C, Schmitz S, Wang F, Sellers JR: **Load-dependent kinetics of myosin-V can explain its high processivity**. *Nat Cell Biol* 2005, **7**:861-869.

7. Wang F, Chen L, Arcucci O, Harvey EV, Bowers B, Xu Y, Hammer JA 3rd, Sellers JR: **Effect of ADP and ionic strength on the kinetic and motile properties of recombinant mouse myosin V**. *J Biol Chem* 2000, **275**:4329-4335.

8. Trybus KM, Krementsova E, Freyzon Y: **Kinetic characterization of a monomeric unconventional myosin V construct**. *J Biol Chem* 1999, **274**:27448-27456.

9. Homma K, Saito J, Ikebe R, Ikebe M: **Ca^{2+}-dependent regulation of the motor activity of myosin V**. *J Biol Chem* 2000, **275**:34766-34771.

10. Mehta AD, Rock RS, Rief M, Spudich JA, Mooseker MS, Cheney RE: **Myosin-V is a processive actin-based motor**. *Nature* 1999, **400**:590-593.

11. •• Lu H, Krementsova E, Trybus KM: **Regulation of myosin V processivity by calcium at the single-molecule level**. *J Biol Chem* 2006, **281**:31987-31994.
Myosin-V was originally discovered to have a peculiar disconnect between ATPase activity and motility in high [Ca^{2+}]. ATPase activity is high in high [Ca^{2+}] but motility is low. This study goes a long way toward explaining this oddity by showing that Ca^{2+} causes premature stoppage of processive runs. Levels of regulation for myosin-V have always been low by steady state ATPase assays of the inactive state and this study explains nicely the 8-fold level observed in many labs. This study also shows the highest levels of regulation so far obtained, which were measured using single turnover kinetics, but the levels are still low by the standards of muscle myosin-II.

12. Trybus KM: **Assembly of cytoplasmic and smooth muscle myosins**. *Curr Opin Cell Biol* 1991, **3**:105-111.

13. Sellers J: **Mechanism of the phosphorylation-dependent regulation of smooth muscle heavy meromyosin**. *J Biol Chem* 1985, **260**:15815-15819.

14. Tauhata SB, dos Santos DV, Taylor EW, Mooseker MS, Larson RE: **High affinity binding of brain myosin-Va to F-actin induced by calcium in the presence of ATP**. *J Biol Chem* 2001, **276**:39812-39818.

15. Yengo CM, De La Cruz EM, Safer D, Ostap EM, Sweeney HL: **Kinetic characterization of the weak binding states of myosin V**. *Biochemistry* 2002, **41**:8508-8517.

16. Berger CL, Thomas DD: **Rotational dynamics of actin-bound intermediates in the myosin ATPase cycle**. *Biochemistry* 1991, **30**:11036-11045.

17. De La Cruz EM, Wells AL, Rosenfeld SS, Ostap EM, Sweeney HL: **The kinetic mechanism of myosin V**. *Proc Natl Acad Sci U S A* 1999, **96**:13726-13731.

18. Martin SR, Bayley PM: **Calmodulin bridging of IQ motifs in myosin-V**. *FEBS Lett* 2004, **567**:166-170.

19. Terrak M, Wu G, Stafford WF, Lu RC, Dominguez R: **Two distinct myosin light chain structures are induced by specific variations within the bound IQ motifs-functional implications**. *EMBO J* 2003, **22**:362-371.

20. Koide H, Kinoshita T, Tanaka Y, Tanaka S, Nagura N, Meyer zu Horste G, Miyagi A, Ando T: **Identification of the single specific IQ motif of myosin V from which calmodulin dissociates in the presence of Ca^{2+}**. *Biochemistry* 2006, **45**:11598-11604.

21. • Wang F, Thirumurugan K, Stafford WF, Hammer JA, 3rd, Knight PJ, Sellers JR: **Regulated conformation of myosin V**. *J Biol Chem* 2004, **279**:2333-2336.
This paper was the first to report the folded conformation of myosin-V in the inactive state obtained at low [Ca^{2+}] and some of its characteristics. Electron micrographs of the 14S conformation preserved in negative stain show the cargo binding domain folded back on the motor domain.

22. • Li XD, Mabuchi K, Ikebe R, Ikebe M: **Ca^{2+}-induced activation of ATPase activity of myosin Va is accompanied with a large conformational change**. *Biochem Biophys Res Commun* 2004, **315**:538-545.
The third of the original studies into the structure of the myosin-V inactive conformation.

23. •• Liu J, Taylor DW, Krementsova EB, Trybus KM, Taylor KA: **Three-dimensional structure of the myosin V inhibited state by cryoelectron tomography**. *Nature* 2006, **442**:208-211.
This paper reports the first 3D structure of the 14S conformation. The 3D reconstruction was obtained using cryoelectron tomography, which is a new and emerging 3D imaging technique. This paper is notable for several technical advances — including a computational correction for the defocus gradient in tilted specimens and the use of correspondence analysis to characterize structure variability — and for the resolution achieved, 2.4 nm, which is high for this 3D imaging technique.

24. Lucic V, Forster F, Baumeister W: **Structural studies by electron**
• **tomography: from cells to molecules**. *Annu Rev Biochem* 2005, **74**:833-865.
Probably the best recent review published on the technique of electron tomography. It is a great starting place for readers unfamiliar with the method.

25. Sweeney HL, Rosenfeld SS, Brown F, Faust L, Smith J, Xing J, Stein LA, Sellers JR: **Kinetic tuning of myosin via a flexible loop adjacent to the nucleotide binding pocket**. *J Biol Chem* 1998, **273**:6262-6270.

26. Olivares AO, Chang W, Mooseker MS, Hackney DD,
•• De La Cruz EM: **The tail domain of myosin Va modulates actin binding to one head**. *J Biol Chem* 2006, **281**:31326-31336.
The first study to report that nucleotide exchange in the 14S inhibited conformation is slowed, even when bound to actin. It also shows that in ADP only one head of the 14S conformation can bind actin strongly; the second head has highly reduced affinity, suggesting that internal motions in the 14S conformation are of high enough amplitude to place both heads on one actin filament, but that the second head binds with much weaker affinity than the first.

27. Thirumurugan K, Sakamoto T, Hammer JA, Sellers JR, Knight PJ:
•• **The cargo-binding domain regulates structure and activity of myosin 5**. *Nature* 2006, **442**:212-215.
This is the second detailed study on the structure of the 14S conformation. Averaged 2D projections images of 14S myosin-V are obtained from micrographs of negatively stained specimens under several sets of conditions, all of which showed similar structures, but the specimens formed in the presence of ATP had low affinity for F-actin.

28. Wendt T, Taylor D, Trybus KM, Taylor K: **Three-dimensional image reconstruction of dephosphorylated smooth muscle heavy meromyosin reveals asymmetry in the interaction between myosin heads and placement of subfragment 2**. *Proc Natl Acad Sci U S A* 2001, **98**:4361-4366.

29. Liu J, Wendt T, Taylor D, Taylor K: **Refined model of the 10S conformation of smooth muscle myosin by cryo-electron microscopy 3D image reconstruction**. *J Mol Biol* 2003, **329**:963-972.

30. Liu Y, Eisenberg D: **3D domain swapping: as domains continue to swap**. *Protein Sci* 2002, **11**:1285-1299.

31. Pashkova N, Jin Y, Ramaswamy S, Weisman LS: **Structural basis**
•• **for myosin V discrimination between distinct cargoes**. *Embo J* 2006, **25**:693-700.
This is the first crystal structure of a cargo binding domain of myosin-V. The structure is that of the yeast myo2 cargo binding domain and shows two domains that share a long α-helix. Mutations that affect secretory vesicle transport and vacuole inheritance mapped to separate domains in the crystal structure.

32. Li XD, Jung HS, Mabuchi K, Craig R, Ikebe M: **The globular tail**
•• **domain of myosin Va functions as an inhibitor of the myosin Va motor**. *J Biol Chem* 2006, **281**:21789-21798.
This interesting study used a monomeric construct of the cargo binding domain, which is usually dimeric in the full length molecule, and rod domain truncation mutants to examine interactions between cargo binding domain and rod in the 14S conformation. They obtained the surprising result that the regions of rod that are close to the cargo binding domain are not important, and that regions near the PEST site are much more important. The result suggests that these regions of rod from the PEST site on are undergoing some significant rearrangements in the 14S conformation.

33. Wang FS, Wolenski JS, Cheney RE, Mooseker MS, Jay DG: **Function of myosin-V in filopodial extension of neuronal growth cones**. *Science* 1996, **273**:660-663.

34. Espreafico EM, Cheney RE, Matteoli M, Nascimento AA, De Camilli PV, Larson RE, Mooseker MS: **Primary structure and cellular localization of chicken brain myosin-V (p190), an unconventional myosin with calmodulin light chains**. *J Cell Biol* 1992, **119**:1541-1557.

35. Star EN, Kwiatkowski DJ, Murthy VN: **Rapid turnover of actin in dendritic spines and its regulation by activity**. *Nat Neurosci* 2002, **5**:239-246.

36. Langford GM: **Myosin-V, a versatile motor for short-range vesicle transport**. *Traffic* 2002, **3**:859-865.

37. Berg JS, Cheney RE: **Myosin-X is an unconventional myosin that undergoes intrafilopodial motility**. *Nat Cell Biol* 2002, **4**:246-250.

38. Kovacs M, Wang F, Sellers JR: **Mechanism of action of myosin**
• **X, a membrane-associated molecular motor**. *J Biol Chem* 2005, **280**:15071-15083.
This very nice study determines kinetic constants for monomeric myosin-X and does so at near physiological ionic strength. They make the surprising observation that myosin-X actin affinity in the strong binding states is much weaker than for corresponding states of other myosins, both muscle and unconventional.

39. Adio S, Reth J, Bathe F, Woehlke G: **Regulation mechanisms of Kinesin-1**. *J Muscle Res Cell Motil* 2006, **27**:153-160.

40. Mogilner A, Rubinstein B: **The physics of filopodial protrusion**. *Biophys J* 2005, **89**:782-795.

41. Lin CH, Forscher P: **Growth cone advance is inversely proportional to retrograde F-actin flow**. *Neuron* 1995, **14**:763-771.